OXFORD

SOT | Society of Toxicology
www.toxsci.oxfordjournals.org

TOXICOLOGICAL SCIENCES, 151(1), 2016, 35–43

doi: 10.1093/toxsci/kfw020
Advance Access Publication Date: January 27, 2016
Research Article

Immunomodulation By Subchronic Low Dose 2,3,7,8-Tetrachlorodibenzo-*p*-Dioxin in Experimental Autoimmune Encephalomyelitis in the Absence of Pertussis Toxin

Eun-Ju Yang, John V. Stokes, Evangel Kummari, Jeffrey Eells, and Barbara L.F. Kaplan[1]

Center for Environmental Health Sciences, Department of Basic Sciences, College of Veterinary Medicine, Mississippi State University, Mississippi 39762

[1]To whom correspondence should be addressed at Center for Environmental Health Sciences, Department of Basic Sciences, College of Veterinary Medicine, Mississippi State University, Mississippi 39762. Fax. 662-325-8884. E-mail: barbara.kaplan@msstate.edu.

ABSTRACT

Multiple sclerosis (MS) is an autoimmune neurodegenerative disorder, characterized by demyelination of neurons in the central nervous system. To investigate the pathogenicity of various T cell types in MS, especially IFN-γ- or IL-17-producing $CD4^+$ cells (T_H1 or T_H17 cells, respectively), the mouse model, experimental autoimmune encephalomyelitis (EAE), is commonly used. One method by which EAE is induced is immunization with myelin oligodendrocyte glycoprotein (MOG) peptide (MOG_{35-55}) followed by subsequent injections of pertussis toxin (PTX) as an adjuvant. We have an interest in the mechanisms by which EAE occurs in the absence of PTX because it induces a milder disease state more consistent with autoimmune disease onset and PTX inactivates $G_{i/o}$ protein-coupled receptors, many of which contribute to immune homeostasis. Another receptor that plays a role in immune homeostasis is the aryl hydrocarbon receptor (AHR). In fact, the environmental contaminant 2,3,7,8-tetrachlorodibenzo-*p*-dioxin (TCDD) has been shown to attenuate EAE pathogenesis by affecting $CD4^+$ T and regulatory T (Treg) cells in an AHR-dependent manner. However, many of these studies have been conducted with an acute high dose TCDD. Thus, the goal of this work was to investigate the modulation of MOG-specific immune responses with subchronic low dose TCDD (0.1–1.0 μg/kg/d for 12 days) in EAE without PTX. The results demonstrate that subchronic, low dose exposure of TCDD attenuates the immune responses in EAE development in the absence of PTX, which is due in part to suppression of MOG-specific IL-17A and IFN-γ responses.

Key words: TCDD; Tregs; EAE; IL-17; IFN-γ; immunomodulation.

Multiple sclerosis (MS) is a demyelinating inflammatory disorder of the central nervous system (Lassmann, 2010), characterized by loss of vision, imbalance of mobility, cognition impairment, and paralysis (Legroux and Arbour, 2015). Many studies have determined that the infiltration of $CD4^+$IFN-γ^+ (T_H1) and $CD4^+$IL-17^+ (T_H17) lymphocytes against myelin self-antigens plays a crucial role in MS pathogenesis (Fletcher *et al.*, 2010). The mechanisms by which these T cells become active is not clear, but it has been suggested that MS incidence can be affected by viral infections, smoking, sunlight (Koch *et al.*, 2013), and various ligands of aryl hydrocarbon receptor (AHR), especially 2,3,7,8-tetrachlorodibenzo-*p*-dioxin (TCDD) and 6-formylindolo(3,2-b)carbazole (FICZ) (Duarte *et al.*, 2013; Quintana *et al.*, 2008).

Although both TCDD and FICZ are both AHR agonists, TCDD is a halogenated aromatic hydrocarbon, a widespread and persistent environmental contaminant (Van den Berg et al., 1998), whereas FICZ is a tryptophan-derived photoproduct that acts as

an endogenous AHR agonist (Rannug *et al.*, 1987). Initial studies demonstrated that they exhibited opposite effects in experimental autoimmune encephalomyelitis (EAE): TCDD potently suppressed, while FICZ exacerbated, disease (Quintana *et al.*, 2008; Veldhoen *et al.*, 2008). Specifically, AHR activation by TCDD showed that the proportion of forkhead box $P3^+$ ($FOXP3^+$) Treg cells was increased whereas those of T_H1 and T_H17 cells were significantly decreased (Quintana *et al.*, 2008). In contrast, FICZ did not increase the number of $CD4^+FOXP4^+$ Treg cells, and the numbers of $CD4^+$ IL-$17A^+$ and $CD4^+$ IL-22^+ T cells were increased, thereby EAE pathogenesis was exacerbated (Veldhoen *et al.*, 2008). More recent studies have demonstrated that FICZ can attenuate disease if administered systemically (Duarte *et al.*, 2013), as opposed to being delivered locally in the antigen emulsion (Veldhoen *et al.*, 2008). The study by Duarte *et al.* (2013) also demonstrated that if TCDD was administered after EAE disease initiation, it was not effective in suppressing EAE. Together these results suggest that the influence of AHR agonist exposure on EAE disease incidence is not yet understood.

Thus, the goal of our study was to determine the effect of low level TCDD exposure on myelin oligodendrocyte glycoprotein (MOG)-induced T cell responses. In several previous reports, TCDD was administered intraperitoneally at 1 μg/mouse (Duarte *et al.*, 2013; Quintana *et al.*, 2008), but we administered TCDD orally at 0.1 or 1.0 μg/kg/d for 12 days for a cumulative TCDD dosage of 0.024–0.24 μg/mouse. Moreover, we induced EAE with MOG peptide in the absence of pertussis toxin (PTX), which we believe more closely mimics MS it results in less severe disease, similar to an early diagnosis in MS. Despite the modest clinical signs, MOG-specific immune responses were readily detectable in the spleen and were modulated by TCDD. Specifically, splenocytes (SPLCs) were analyzed for T-cell subsets including Treg, $CD4^+$, $CD8^+$, and $\gamma\delta$ TCR^+ cells.

MATERIALS AND METHODS

Mice

Female C57BL/6 mice were obtained from Harlan Laboratories (Indianapolis, Indiana) at 5–8 weeks of age. Animal experiments and maintenance were approved by Mississippi State University Institutional Animal Care and Use Committee according to AAALAC guidelines. All animals were housed 3–5 to a cage and maintained in a sterile, temperature (22 ± 1 °C) and light controlled (12-h light: 12-h dark) room, and provided with food and water ad libitum.

EAE Induction, TCDD Administration and Clinical Assessment

Mice were immunized with 100 μg of mouse MOG peptide (MOG_{35-55}, MEVGWYRSPFSRVVHLYRNGK, Biosynthesis, Lewisville, Texas) emulsified in complete Freund's adjuvant (CFA, Sigma, Saint Louis, Missouri) supplemented with 4 mg/ml heat-killed *Mycobacterium tuberculosis* H37Ra (HKMT, BD Biosciences, Detroit, Michigan). Prepared MOG emulsion was injected on 4 flanks of the mice (2 shoulders and 2 hips at 25 μl each). TCDD (AccuStandard, New Haven, Connecticut) was dissolved in corn oil (CO, Sigma) to make a stock solution and the stock was further diluted with CO before administration. From the first day postimmunization, mice were administered CO or TCDD (0.1 or 1 μg/kg/d) for 12 days by oral gavage, which allowed for examination of subchronic TCDD exposure in the time preceding clinical signs. The body weight and clinical score of mice were recorded at least every 2 days. The EAE clinical signs were observed and recorded as follows: 0, healthy; 1, flaccid tail; 2, impaired righting reflex and/or gait; 3, partial hind limb paralysis; 4, total hind limb paralysis. Mice were not allowed to progress beyond a clinical score of 4 at any time. Results are averaged or are representative from 2 to 4 separate experiments as noted in the figure legends. The data obtained at end-stage disease are denoted as 'late', typically necropsied on day 18 (about 25% of EAE + CO mice reached a clinical score of 4 before day 18 and were necropsied at that time and analyzed with the rest of the day 18 samples). All data obtained "early" were from mice necropsied on day 3; thus mice only received TCDD on days 1–2 after EAE immunization on day 0 for the day 3 timepoint.

RNA Isolation and cDNA Synthesis

One lobe of liver or half of the spleen was collected and stored in 1 ml TRI reagent (Sigma-Aldrich) at −80 °C until use. Samples were allowed to thaw on ice, homogenized, then 0.2 ml 1-bromo-3-chloropropane (Sigma-Aldrich) was added, and mixed thoroughly for 15 s. After incubation for 15 min at room temperature (RT), samples were centrifuged (12 000 × *g*, 5 min, 4 °C) to break the aqueous and organic phases. The clear top aqueous layer was transferred to a fresh tube and RNA was precipitated with 0.5 ml isopropanol. Samples were mixed and incubated for 10 min at RT, centrifuged (12 000 × *g*, 10 min, 4 °C) and the supernatant discarded. The collected pellet was then applied to the SV Total RNA Isolation System (Promega, Madison, Wisconsin) according to the manufacturer's instructions. Isolated RNA was quantified and adjusted to same quantity for whole samples by using molecular biology grade water (DNase, RNase, and protease-free, Corning Life Sciences, Manassas, Virginia). To synthesize complementary DNA (cDNA), high capacity cDNA Reverse Transcription Kit (Applied Biosynthesis, Foster City, California) was used. Samples were run on a thermal cycler (25 °C for 10 min, 37 °C for 120 min, 85 °C for 10 s, then hold at 4 °C) and synthesized cDNA was stored at −20 °C until analysis of quantitative real time-polymerase chain reaction (qRT-PCR).

qRT-PCR Analysis

Synthesized cDNA (8 μl) was mixed with 32 μl primer mix solution (8 μl water, 2 μl 18s rRNA primer [probe dye VIC-MGB], 2 μl of 20 × Taqman primer/probe set [Mm 00487218_m1 *Cyp1a1*, Applied Biosystems, Foster City, California], and 20 μl of 2 × Taqman Universal Master Mix [Applied Biosystems]). To remove bubbles, PCR strips were centrifuged at 100 × *g* for 10 s. *Cyp1a1* mRNA expression was analyzed with an Mx3005p qPCR system (Agilent Technologies, Santa Clara, California). Data were analyzed by the ΔΔCt method with 18s rRNA as the endogenous reference (Livak and Schmittgen, 2001; Thellin *et al.*, 1999). mRNA expression levels were expressed as fold change.

SPLC isolation and MOG peptide restimulation

The spleen was placed in a 6-well plate and mechanically disrupted in 1 ml of serum-free 1 × Roswell Park Memorial Institute (RPMI) 1640 media (Gibco, Grand Island, New York). To remove the insoluble tissue, the solution was allowed to settle and the supernatant containing the single cells was collected. Cells were centrifuged at 400 × *g* for 5 min at RT. The SPLC pellet was resuspended in 1 ml culture media and counted on a Coulter Counter (Beckman Coulter, Indianapolis, Indiana) in the presence of Zapoglobin to lyse red blood cells. For T-cell culture, 1 × RPMI 1640 supplemented with 2% bovine calf serum

(HyClone, Logan, Utah), 29.8 mM sodium bicarbonate ($NaHCO_3$), 100 U penicillin/ml (Gibco), 100 μg streptomycin/ml (Gibco), and 50 μM 2-β-mercaptoethanol (2-ME, Gibco) was used. Isolated SPLCs were seeded at a density of 1×10^6 cells/well in 48-well plates and incubated in a humidified atmosphere at 5% CO_2 and 37 °C. After 30 min, cells were untreated or restimulated with 100 μg/ml MOG peptide for overnight. The following day, the supernatants were collected for enzyme-linked immunosorbent assays to quantify the cytokine production and MOG peptide-restimulated cells were resuspended in 5 μg/ml brefeldin A (BioLegend, San Diego, California)-containing RPMI without serum for 4 h for flow cytometry analysis.

Flow Cytometry and Gating Strategy

Cell surface marker staining

Treg cells were stained on the day of necropsy, but intracellular cytokines from T cells were stained after overnight restimulation with MOG peptide. Cell staining was performed in 12 × 75 mm tubes (BD Falcon, Franklin Lakes, New Jersey). Cells were washed once with 1 × PBS, centrifuged at 500 × *g* for 5 min at RT, and the supernatant was discarded. Then they were incubated with Fixable Viability Dye eFluor 780 (FVD, eBiosciences, San Diego, California) for 30 min at 4 °C to collect live cells via negative fluorescence intensity of FVD. After washing the cells with 1 × PBS and fluorescence-activated cell sorting (FACS) buffer (Hank's Balanced Salt Solution containing 1% bovine serum albumin [BSA], pH 7.3) once each, cells were treated with mouse Fc block (purified antimouse CD16/CD32, clone 2.4G2, BD Biosciences) for 15 min at RT to avoid nonspecific binding followed by labeling with the fluorescently conjugated antibodies for surface markers in the dark for 30 min at RT. The antibodies used for staining of cell surface markers are as follows (all antibodies were purchased from BioLegend except where noted): Treg cells, PE/Cy7 anti-CD4 (clone GK1.5) and FITC anti-CD25 (clone PC61.5, eBioscience); T cells, PE/Cy5 anti-CD4 (clone GK1.5), PE/Cy7 anti-CD8α (clone 53-6.7), and FITC anti-TCRγδ (clone GL3). These antibodies were delivered in 50 μl of FACS buffer. Cells were washed with FACS buffer and fixed using Cytofix (BD Biosciences). After 15 min, fixed cells were washed with FACS buffer and stored at 4 °C until intracellular staining. Treg cells were immediately fixed and permeabilized using FOXP3 staining kit (eBioscience).

Intracellular marker staining

After cell surface staining, cells were washed once with permeabilization buffer. Then they were incubated with 50 μl permeabilization buffer for 15 min at RT followed by antibody labeling for 1 h in the dark. Cells were washed with 1 ml permeabilization buffer and resuspended in 400 μl FACS buffer for flow cytometry analysis. Cells were analyzed the same day as intracellular staining. The antibodies used for intracellular markers staining are as follows (all antibodies were purchased from BioLegend except where noted): Treg cells, APC anti-FOXP3 (clone FJK-16S, eBioscience); T cells, APC anti-IL-17A (clone TC11-18H10), PE eFluor 610 anti-IFN-γ (clone XMG1.2). These antibodies were delivered in 50 μl permeabilization buffer.

Flow Cytometry Analysis

Stained cells were acquired on FACSAria III (BD Biosciences) and data analysis was performed using FlowJo (FlowJo, LLC, Ashland, Oregon) software. Dead cells were excluded using high fluorescence intensity of FVD and forward scatter characteristics. To identify the cell types, additional gating was created for Treg cells (CD25 and FOXP3 within CD4) and T cells (IL-17A and IFN-γ within CD4, CD8, or TCRγδ). TCRγδ population was gated from the CD4 and CD8 double negative population as to avoid double reporting any cytokine production from $CD4^+$ or $CD8^+$ since TCRγδ expression in SPLC can be low. Bead controls were prepared for compensation, and fluorescence minus one cell controls were used to establish the gating for every fluorochrome in the staining mixture.

Enzyme-Linked Immunosorbent Assay

For quantification of extracellular cytokines (IL-17A, IFN-γ, IL-6, and IL-2), plates were coated with 0.5–1 μg/ml purified antibodies against IL-17A (clone TC11-18H10.1, BioLegend), IFN-γ (clone AN-18, BioLegend), IL-6 (clone MP5-20F3, BioLegend), or IL-2 (clone JES6-1A12, BioLegend) in coating buffer (0.1 M carbonate-biocarbonate buffer, pH 9.6). After an overnight incubation at 4 °C, the plate was washed with 0.05% Tween-20 in PBS (pH 7.4) and deionized water 3 times each. The plate was blocked with 3% BSA-containing PBS for 1 h at RT. After washing the plate, serum or T-cell culture supernatants were added to wells and incubated for 1 h. After another wash, plate was incubated with 0.5–1 μg/ml biotin-conjugated antibodies against IL-17A (clone TC11-8H4, BioLegend), IFN-γ (clone R4-6A2, BioLegend), IL-6 (clone MP5-32C11, BioLegend), or IL-2 (clone JES6-5H4, BioLegend) for 1 h. Then the plate was washed and treated with 100 μl of Avidin-conjugated with horseradish peroxidase (HRP-Avidin; 1:500 dilution in 3% BSA-containing PBS, BioLegend) in the dark. After 1 h, unbound HRP-Avidin was removed by plate washing, and 3,3′5,5′-tetramethylbenzidine substrate set (BioLegend) was used for blue color development. To stop the color development, 100 μl of 2 N sulfuric acid (H_2SO_4) was added for endpoint assay (optical density at 450 nm) by a microplate reader (SpectraMax M5, Molecular Devices, Sunnyvale, California). To generate a standard curve for cytokine quantification, recombinant standards for IL-17A, IFN-γ, IL-6, or IL-2 were obtained from BioLegend.

Immunohistochemistry in the Spinal Cord

Spinal columns were fixed in 10% normal buffered formalin. Spinal cords were dissected then paraffin-embedded. 5-μm sections of the lumbar enlargement were stained with hematoxylin and eosin (H&E) or luxol fast blue to assess inflammation or demyelination, respectively. The degree of inflammation was scored blindly by 2 separate individuals on a scale from 1 to 4 using 3 images at 40× of different sections from each mouse. Inflammation scores were averaged from the 2 individuals and a regression analysis was performed to determine the correlation between inflammation score and clinical score.

Statistical Analysis

Statistical analysis was performed using GraphPad Prism 6 (GraphPad software). Percent and fold change data were transformed prior to ANOVA analysis. Comparisons were calculated by 1- or 2-way ANOVA followed by a *post hoc* test for multiple comparisons. One-way ANOVA was conducted when evaluating TCDD's effect in EAE only and typically Dunnett's *post hoc* test was performed using EAE + CO as the comparison group (eg, disease onset and area under the curve clinical score). Two-way ANOVA was performed when comparing TCDD's effect in saline (SAL) versus EAE mice and Tukey's multiple comparison test

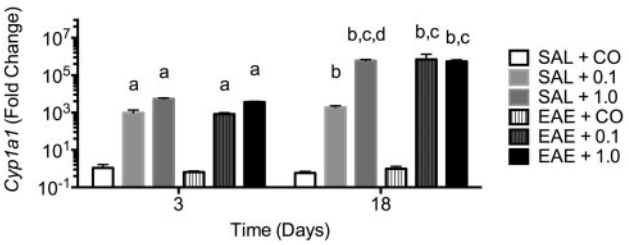

FIG. 1. *Cyp1a1* mRNA expression in early and late stages of pathogenic progression. Total RNA was isolated from liver ($n \geq 3$) and qRT-PCR was used to assess *Cyp1a1* mRNA levels. Data are expressed as mean ± SD. Letters indicate statistical significance at $P < .05$. a, different from SAL + CO at day 3; b, different from SAL + CO at day 18; c, different as compared with same group at day 3; d, different as compared with SAL + 0.1 at day 18. 0.1 and 1.0 denote μg/kg/d TCDD.

was used as the *post hoc* test. In all cases, the level of significance was defined as $P < 0.05$.

RESULTS

Cyp1a1 mRNA Expression in Spleen and Liver

To confirm effective TCDD delivery following oral gavage, *Cyp1a1* mRNA expression was assessed in the liver and spleen. As seen in Figure 1, *Cyp1a1* expression was robustly induced in liver after only 2 days of dosing and the high expression level was maintained through end-stage disease even though TCDD dosing had been discontinued 6 days earlier. EAE disease induction did not alter *Cyp1a1* expression. *Cyp1a1* mRNA expression in the spleen was not significantly increased at any time (data not shown).

Clinical Signs during EAE Development

The clinical signs of CO-administered EAE mice (EAE + CO) first appeared at day 14, and reached a peak level around day 18. Although some mice progressed to dual hind limb paralysis (clinical score 4), most mice only exhibited loss of tail tone and awkward gait by day 18 (clinical score 0.5–1.5). SAL-injected mice, even those treated with TCDD, exhibited no clinical symptoms. TCDD at both 0.1 and 1.0 μg/kg/d exhibited modest reduction of EAE-induced clinical signs and statistically significant delay in disease onset (Table 1). Mice also experienced weight loss that correlated with clinical signs. Thus, EAE + CO and EAE + 0.1 μg/kg/d TCDD produced modest weight gain, which was due in part to some animals losing weight, but the weight of EAE mice treated with 1.0 μg/kg/d TCDD was similar to SAL-treated mice (Table 1). Spinal cord inflammation and demyelination was assessed by H&E and luxol fast blue staining, respectively, and demonstrated increased inflammation and damage to the white matter tracts in response to EAE + CO, which was reduced in response to EAE + TCDD 1.0 μg/kg/d (Figure 2). A linear regression analysis of inflammation score and clinical score resulted in a R^2 value of 0.8517.

Assessment of TCDD Effect on Splenic Treg and T-Cell Subsets

The first T-cell population that was evaluated in the spleen was $CD4^+CD25^+FOXP3^+$ Treg cells in order to determine the generation of Treg cells in response to TCDD in this lower dose range. Tregs were assessed at both early and late disease stages. At day 3, the Treg proportion was not changed by EAE, nor was it altered by the higher dose of TCDD (Figure 3A). However, Treg cells were significantly increased by 0.1 and 1.0 μg/kg/d TCDD compared with EAE + CO by day 18 (Figure 3B). This TCDD effect is consistent with other reports in which increased Treg cells is related to TCDD-induced inhibition of EAE (Quintana *et al.*, 2008).

Next, the responses of various T cells after restimulation with 100 μg/ml MOG were determined at day 18. All splenic T-cell populations ($CD4^+$, $CD8^+$ and $\gamma\delta^+$ T cells) were reduced in EAE mice. Neither dose of TCDD significantly affected the T-cell proportions, although there was a trend toward suppression of the $\gamma\delta^+$ T-cell population (Figure 4A). Within the $CD4^+$ T-cell population, the proportion of IL-$17A^+$IFN-γ^- (T_H17) and IL-$17A^-$IFN-γ^+ (T_H1) cells were slightly increased in EAE + CO as compared with SAL-treated mice, indicating antigen specificity. TCDD suppressed T_H1 cells regardless of disease in a dose-dependent manner (Figure 4B). Although there was no significant elevation of IL-17A or IFN-γ in the $CD8^+$ population in response to MOG restimulation in EAE mice, TCDD did suppress the IL-$17A^+$IFN-γ^- population in $CD8^+$ T cells (Figure 4C). In $\gamma\delta^+$ T cells, EAE induction significantly induced the IL-$17A^+$IFN-γ^- population, which was suppressed by TCDD especially in the absence of disease (Figure 4D). It should be noted that while TCDD consistently suppressed intracellular IFN-γ in $CD4^+$ cells, the effects on IL-17A were more variable across our studies. For instance, we observed no effect of TCDD on intracellular IL-17A in $CD8^+$ cells in one of our studies, but in this study, TCDD suppressed the IL-$17A^+$IFN-γ^- population in $CD8^+$ T cells. Together, these data suggest that intracellular IFN-γ is a more sensitive target of suppression of TCDD as compared with intracellular IL-17A.

Quantification of Various Cytokine Production in Serum and Supernatants

TCDD produced no significant effect on circulating IL-17A levels in serum, but produced a modest effect on circulating IFN-γ (Figure 5). Despite the variability of TCDD's effects on IL-17A, TCDD consistently and robustly suppressed IL-17A release from MOG-stimulated SPLC at end-stage disease (Figure 6). Moreover, TCDD also significantly reduced the production of MOG-specific IFN-γ, IL-6, and IL-2 (Figure 6). No significant cytokine production was induced in the absence of MOG (data not shown), nor did TCDD induce any cytokine release in SAL-treated mice.

DISCUSSION

The mechanisms by which MS occurs are not understood but have been associated with previous bacterial, parasitic, or viral infections, exposure to UV radiation, smoking or other environmental contaminant exposure (Koch *et al.*, 2013). In the case of EAE following exposure to AHR ligands, the data have been inconsistent thus far. Early studies in which AHR was identified as a critical regulator of T_H17 cells in the EAE model demonstrated that a single high dose of TCDD administered at disease initiation (Quintana *et al.*, 2008) or 2 injections 1 day prior and on the day of immunization (Hanieh and Alzahrani, 2013) attenuated EAE clinical scores concomitant with inhibition of IL-17 and IFN-γ in $CD4^+$ T cells and an increase in $CD4^+FOXP3^+$ Tregs. On the other hand, FICZ administered as a systemic high dose (Quintana *et al.*, 2008) or as a local lower dose (Veldhoen *et al.*, 2008) exacerbated EAE. It was shown in the latter case that FICZ increased the number of $CD4^+$IL-17^+ cells but decreased $CD4^+FOXP3^+$ cells (Veldhoen *et al.*, 2008). Additional studies demonstrated that TCDD at lower doses (Quintana *et al.*, 2008)

TABLE 1. EAE Disease Course

Group	Incidence[a]	Onset[b]	% BW Δ[c]	End Clinical Score[d]	AUC Clinical Score[e]
SAL + CO	0/12	N/A	6.2 ± 4.2	0	N/A
SAL + 0.1	0/4	N/A	12.5 ± 5.2	0	N/A
SAL + 1.0	0/4	N/A	9.6 ± 3.6	0	N/A
EAE + CO	11/12	15.0 ± 1.5	2.5 ± 13.0	1.4 ± 1.5	4.0 ± 3.9
EAE + 0.1	3/4	15.5 ± 2.4	0.8 ± 17.2	1.8 ± 2.1	3.0 ± 2.9
EAE + 1.0	6/12	17.9 ± 1.3*	12.2 ± 8.7	0.5 ± 1.1	1.3 ± 3.0

[a]Indicated by a minimum clinical score of 0.5 at any time.
[b]Mean onset day ± SD; mice with no disease incidence are excluded.
[c]BW, body weight; Δ, change; calculated as ([day 1 BW-necropsy BW]/day 1 BW) × 100; mean change ± SD; some animals lost weight in the EAE/CO and EAE/0.1 groups, resulting in a smaller % BW Δ that was still positive.
[d]Mean clinical score at necropsy ± SD.
[e]AUC, area under the curve for clinical score calculated for individual animals; mean AUC ± SD.
*$P < .05$ as compared with EAE/CO.

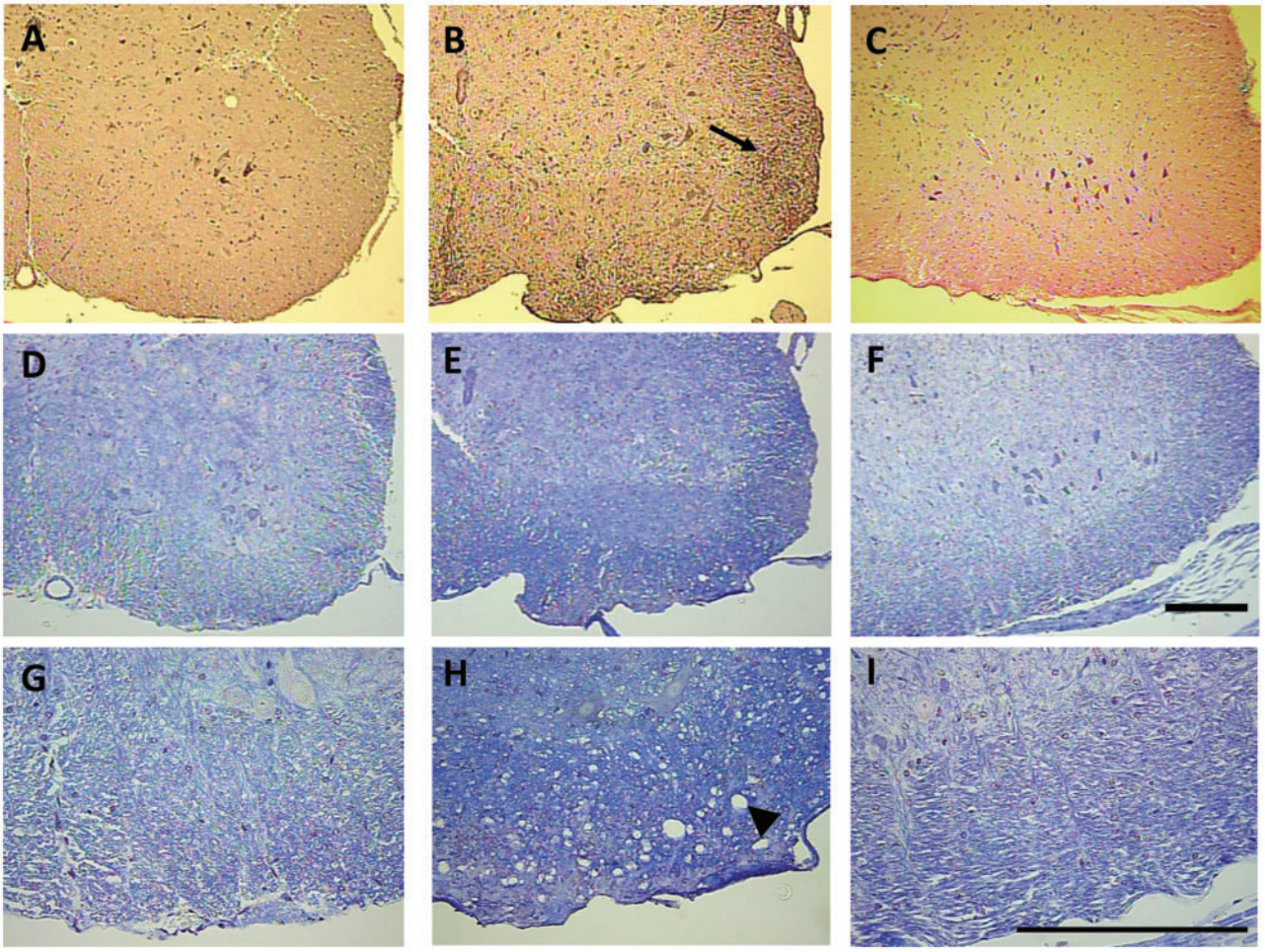

FIG. 2. TCDD reduces spinal cord inflammation and demyelination. Micrographs of H&E **(A–C)** and luxol fast blue staining **(D–I)** in the ventral lumbosacral spinal cord are shown of representative sections from SAL + CO (10×-A,D; 40×-G), EAE + CO (10×-B,E; 40×-H), and EAE + 1.0 (10×-C,F; 40×-I) mice. Inflammatory infiltrates (arrow) in the H&E-stained sections and white matter damage (arrow head) in the luxol fast blue-stained sections are obvious in an EAE + CO mouse that had a clinic score of 4 (B,E,H), but absent in the SAL + CO mice (A,D,G). No noticeable inflammation was observed in the EAE + 1.0 mice (C,F,I). A linear regression analysis of inflammation score and clinical score resulted in a R^2 value of 0.8517. 1.0 denotes μg/kg/d TCDD. Bar = 200 mm.

or administered after EAE initiation (Duarte *et al.*, 2013) produced no effect on EAE clinical score, and that FICZ administered systemically can attenuate EAE (Duarte *et al.*, 2013). Thus, the role of AHR ligation in EAE incidence and severity is not yet understood.

In this study, we examined splenic MOG-specific T cell responses following low dose, subchronic TCDD administration in EAE without PTX. This model more closely mimics the contribution that environmental contaminants make to MS incidence because TCDD was administered at low doses orally, the most

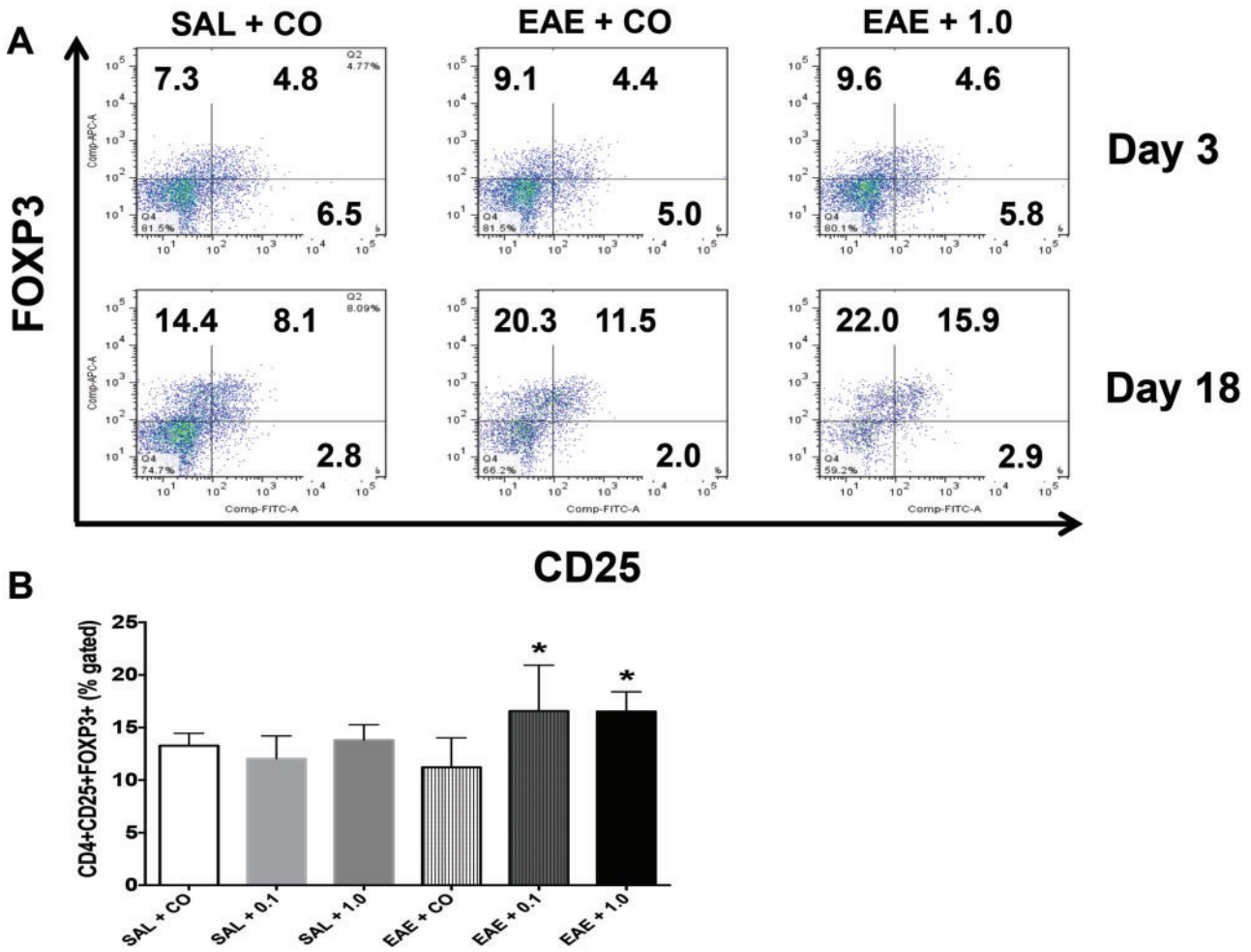

FIG. 3. Increased CD4$^+$CD25$^+$FOXP3$^+$ Treg cells by TCDD at the late stage. **(A)** SPLCs were stained for CD4, CD25 and FOXP3 at early and late stages and analyzed the same day. Dot plots are representative of at least 3 individual mice per group. **(B)** The proportion of CD4$^+$CD25$^+$FOXP3$^+$ Treg cells at late stage ($n = 4$). Data are mean ± SD. *$P < .05$ as compared with EAE + CO. 0.1 and 1.0 denote μg/kg/d TCDD.

likely human exposure paradigm. In addition, we avoid PTX in our EAE model because it allows us to examine the contribution that TCDD makes to a milder disease state, mimicking autoimmune disease onset. PTX also disrupts immune homeostasis at EAE initiation though inhibition of $G_{i/o}$ protein-coupled receptors and induces T_H17 cells in the spleen and lymph nodes (Hofstetter *et al.*, 2007). Since AHR also regulates T_H17 cells (Quintana *et al.*, 2008; Veldhoen *et al.*, 2008), our model allows us to examine the effect of TCDD on IL-17A-producing cells without this potential confound. As a biomarker of exposure, *Cyp1a1* levels were measured in spleen and liver early and late in disease. Consistent with other studies in which TCDD was sequestered in the liver (Santostefano *et al.*, 1998), *Cyp1a1* was robustly induced in the liver, but not in the spleen. However, splenic T-cell function was still altered.

Specifically, CD4$^+$ CD25$^+$ FOXP3$^+$ T cells were induced in the spleen by both doses of TCDD late in disease, consistent with other reports that TCDD induces Tregs (Funatake *et al.*, 2005). Importantly, TCDD produced no effect on Tregs in the absence of disease, confirming that Treg induction is one mechanism by which TCDD produced modest reductions in EAE clinical scores.

CD4$^+$IFN-γ$^+$ cells were also consistent targets of suppression by TCDD, and there was a suggestion that TCDD could attenuate IFN-γ in CD8$^+$ T cells. MOG-induced IFN-γ production from SPLC was also significantly suppressed. When compared with other studies in which CD8$^+$T cell responses have been studied (Wheeler *et al.*, 2014), the TCDD-induced CD8$^+$ effects are modest. This could be a result of TCDD dose or tissue. For instance, the number of CD8$^+$IFN-γ$^+$T cells from mediastinal lymph nodes was significantly decreased when mice were infected with influenza A virus after administration with 10 μg TCDD/kg (Wheeler *et al.*, 2014).

In our model the effects on IL-17A were variable. For instance, intracellular IL-17A appeared to be sensitive to suppression by TCDD in EAE, but this was not observed consistently across studies. However, IL-17A release from SPLC was consistently suppressed suggesting TCDD affects IL-17A release, but not necessarily IL-17A production. Alternatively, it is possible the kinetics for intracellular versus released IL-17A are different and TCDD's effects are time-dependent. Finally, the model does induce mild clinical disease; however, even in EAE mice with no clinical score at necropsy exhibited MOG-specific induction of intracellular and released cytokines so we do not believe the mild disease course contributes to variability in the TCDD effect. There was a possibility that TCDD would induce IL-17A production since it has been shown to be critical for T_H17 induction (Quintana *et al.*, 2008; Veldhoen *et al.*, 2008), but we did not observe significant induction of IL-17A as evaluated by

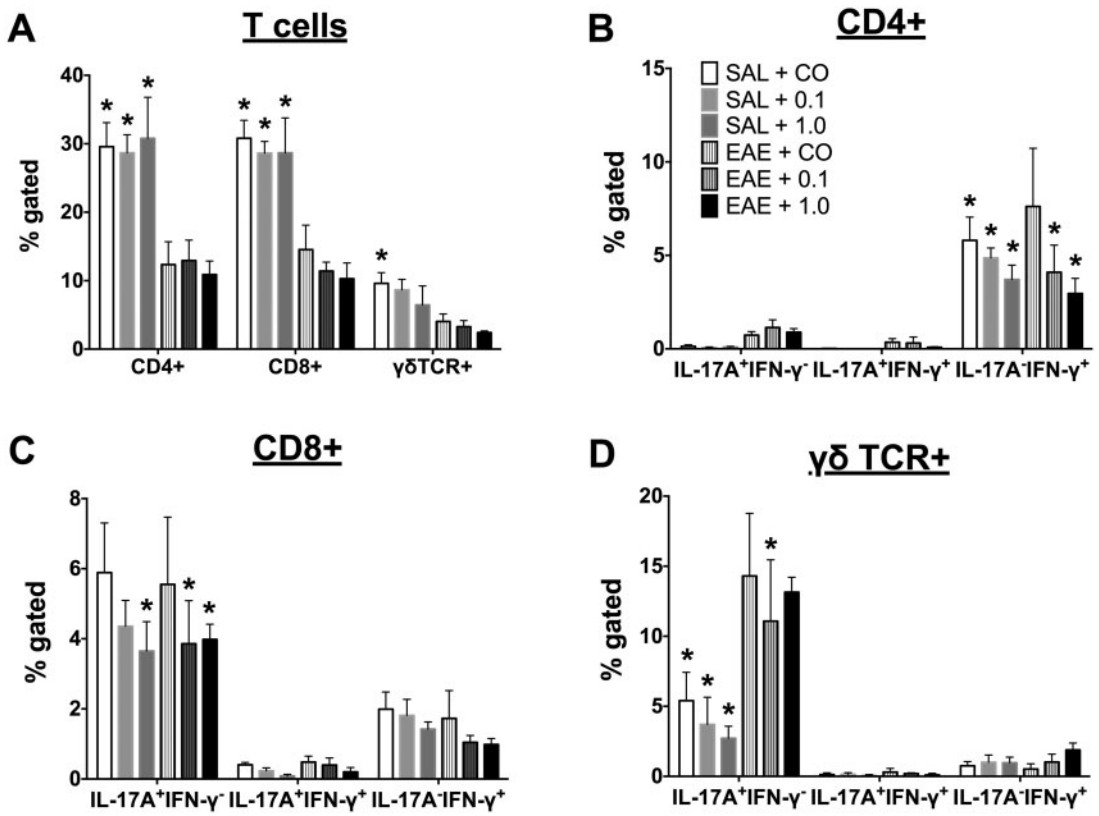

FIG. 4. Modulation of $CD4^+$, $CD8^+$, and γδ TCR^+ splenic T-cell populations by TCDD at the late stage. SPLC ($n = 4$) were cultured overnight with 100 μg/ml MOG peptide after which cells were stained for various T-cell populations, **(A)** T-cell proportions; **(B)** $CD4^+$, **(C)** $CD8^+$, and **(D)** γδ TCR^+ cells. Cells were gated on live lymphocytes. In addition, γδ TCR^+ cells were gated off the $CD4^-CD8^-$ population. Data are mean ± SD. *$P < .05$ as compared with EAE + CO within the population as defined on the x-axis. 0.1 and 1.0 denote μg/kg/d TCDD.

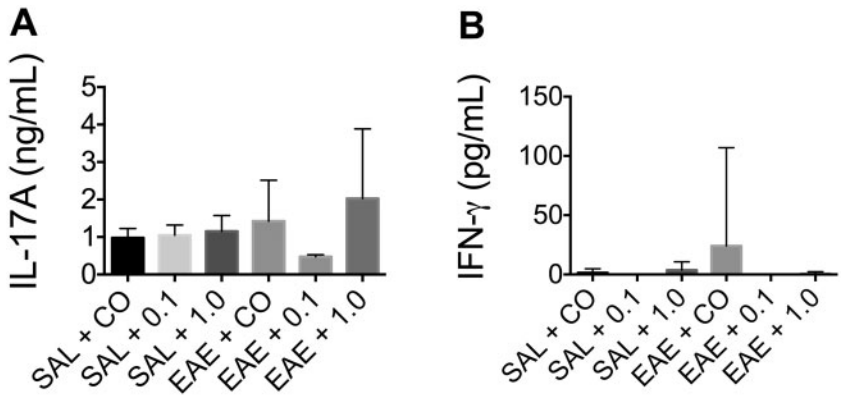

FIG. 5. Effect of TCDD on circulating IL-17A and IFN-γ in serum. Serum was collected from mice ($n \geq 4$) at the late stage and analyzed for cytokine production **(A)** IL-17A; **(B)** IFN-γ. Data are mean ± SD and no statistical significance was detected. 0.1 and 1.0 denote μg/kg/d TCDD.

intracellular staining, circulating in serum, or secreted by MOG peptide-restimulated SPLC.

There was also a modest effect by TCDD on γδ TCR^+ T cells. There was modest suppression of the proportion of γδ TCR^+ expression in disease and by TCDD. It should be emphasized that especially because γδ TCR^+ T cells are low in the spleen, these populations were obtained by gating off the $CD4^-CD8^-$ population to avoid picking up CD4 or CD8 T cells near the negative side of the gate. EAE induced significant IL-17A production in γδ TCR^+ T cells, but there was modest modulation by TCDD.

MOG-specific IL-2 and IL-6 cytokine production was also suppressed by TCDD. These cytokines were not evaluated by flow cytometry and therefore, it is not clear which cell type(s) were affected. IL-2 is produced by mainly T cells, natural killer and dendritic cells (DCs) (Almeida *et al.*, 2006; Malek, 2008; Setoguchi *et al.*, 2005), while IL-6 is mainly produced by macrophages during acute inflammation and by T cells during chronic inflammation (Naugler and Karin, 2008). Recently, there have been some reports about the role of DC in EAE or anti-inflammatory TCDD effect. For instance, Duarte et al. (2013) determined that the immunosuppressive effect of TCDD depends on

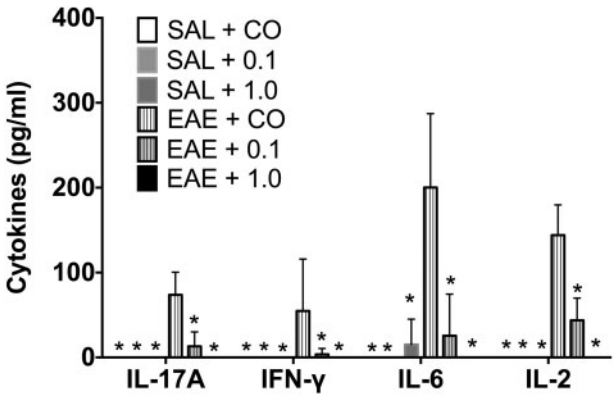

FIG. 6. Reduction of MOG peptide-specific cytokine production by SPLC by TCDD at the late stage. SPLCs from mice ($n \geq 4$) were cultured overnight in the absence or presence of 100 μg/ml MOG peptide after which supernatants were analyzed for cytokine production (IL-17A, IFN-γ, IL-6, and IL-2). Data are mean ± SD. *$P < .05$ as compared with EAE + CO within the cytokine group. 0.1 and 1.0 denote μg/kg/d TCDD.

AHR activation, not only in T cells, but also in DC. Also, an endogenous AHR ligand 2-(1′H-indole-3′-carbonyl)-thiazole-4-carboxylic acid methyl ester significantly inhibited mRNA expression of various cytokines including IL-6 in EAE-induced splenic DC (Quintana *et al.*, 2010), and our results demonstrate the effect of low dose TCDD on IL-2 and IL-6-producing cells.

Overall, these results demonstrate that subchronic low dose TCDD alters splenic T cell responses to MOG in EAE without PTX. The primary mechanisms by which TCDD attenuated EAE involved splenic Treg induction and inhibition of IFN-γ production. The results are in contrast with a recent study in which developmental exposure of low dose TCDD to pups via lactation in an autoimmune model exacerbated autoimmune symptoms (Boule *et al.*, 2015). However, TCDD exposure during development as opposed to adulthood has been shown to produce differing effects on T-cell function, including IFN-γ (Hogaboam *et al.*, 2008; Vorderstrasse *et al.*, 2004). Thus, future studies could focus on developmental exposures of different AHR ligands and lymphocyte function in target tissues, such as brain or spinal cord. The strength of these studies is that they demonstrate that subchronic low dose TCDD suppressed splenic T-cell IFN-γ production and induced splenic Tregs in a model of mild (or early onset) MS.

FUNDING

This study was funded by Mississippi State University College of Veterinary Medicine.

REFERENCES

Almeida, A. R., Zaragoza, B., and Freitas, A. A. (2006). Indexation as a novel mechanism of lymphocyte homeostasis: The number of CD4+CD25+ regulatory T cells is indexed to the number of IL-2-producing cells. *J. Immunol.* **177**, 192–200.

Boule, L. A., Burke, C. G., Fenton, B. M., Thevenet-Morrison, K., Jusko, T. A., and Lawrence, B. P. (2015). Developmental activation of the AHR increases effector CD4+ T Cells and exacerbates symptoms in autoimmune disease-prone Gnaq+/- Mice. *Toxicol. Sci.* **148**, 555–566.

Duarte, J. H., Di Meglio, P., Hirota, K., Ahlfors, H., and Stockinger, B. (2013). Differential influences of the aryl hydrocarbon receptor on Th17 mediated responses in vitro and in vivo. *PLoS One* **8**, e79819.

Fletcher, J. M., Lalor, S. J., Sweeney, C. M., Tubridy, N., and Mills, K. H. (2010). T cells in multiple sclerosis and experimental autoimmune encephalomyelitis. *Clin. Exp. Immunol.* **162**, 1–11.

Funatake, C. J., Marshall, N. B., Steppan, L. B., Mourich, D. V., and Kerkvliet, N. I. (2005). Cutting edge: Activation of the aryl hydrocarbon receptor by 2,3,7,8-tetrachlorodibenzo-p-dioxin generates a population of CD4+ CD25+ cells with characteristics of regulatory T cells. *J. Immunol.* **175**, 4184–4188.

Hanieh, H., and Alzahrani, A. (2013). MicroRNA-132 suppresses autoimmune encephalomyelitis by inducing cholinergic anti-inflammation: A new Ahr-based exploration. *Eur. J. Immunol.* **43**, 2771–2782.

Hofstetter, H. H., Grau, C., Buttmann, M., Forsthuber, T. G., Gaupp, S., Toyka, K. V., and Gold, R. (2007). The PLPp-specific T-cell population promoted by pertussis toxin is characterized by high frequencies of IL-17-producing cells. *Cytokine* **40**, 35–43.

Hogaboam, J. P., Moore, A. J., and Lawrence, B. P. (2008). The aryl hydrocarbon receptor affects distinct tissue compartments during ontogeny of the immune system. *Toxicol. Sci.* **102**, 160–170.

Koch, M. W., Metz, L. M., Agrawal, S. M., and Yong, V. W. (2013). Environmental factors and their regulation of immunity in multiple sclerosis. *J. Neurol. Sci.* **324**, 10–16.

Lassmann, H. (2010). Axonal and neuronal pathology in multiple sclerosis: What have we learnt from animal models. *Exp. Neurol.* **225**, 2–8.

Legroux, L., and Arbour, N. (2015). Multiple sclerosis and T lymphocytes: An entangled story. *J. Neuroimmune Pharmacol.* **10**, 528–546.

Livak, K. J., and Schmittgen, T. D. (2001). Analysis of relative gene expression data using real-time quantitative PCR and the 2(-Delta Delta C(T)) Method. *Methods* **25**, 402–408.

Malek, T. R. (2008). The biology of interleukin-2. *Annu. Rev. Immunol.* **26**, 453–479.

Naugler, W. E., and Karin, M. (2008). The wolf in sheep's clothing: The role of interleukin-6 in immunity, inflammation and cancer. *Trends Mol. Med.* **14**, 109–119.

Quintana, F. J., Basso, A. S., Iglesias, A. H., Korn, T., Farez, M. F., Bettelli, E., Caccamo, M., Oukka, M., and Weiner, H. L. (2008). Control of T(reg) and T(H)17 cell differentiation by the aryl hydrocarbon receptor. *Nature* **453**, 65–71.

Quintana, F. J., Murugaiyan, G., Farez, M. F., Mitsdoerffer, M., Tukpah, A. M., Burns, E. J., and Weiner, H. L. (2010). An endogenous aryl hydrocarbon receptor ligand acts on dendritic cells and T cells to suppress experimental autoimmune encephalomyelitis. *Proc. Natl. Acad. Sci. U.S.A.* **107**, 20768–20773.

Rannug, A., Rannug, U., Rosenkranz, H. S., Winqvist, L., Westerholm, R., Agurell, E., and Grafstrom, A. K. (1987). Certain photooxidized derivatives of tryptophan bind with very high affinity to the Ah receptor and are likely to be endogenous signal substances. *J. Biol. Chem.* **262**, 15422–15427.

Santostefano, M. J., Wang, X., Richardson, V. M., Ross, D. G., DeVito, M. J., and Birnbaum, L. S. (1998). A pharmacodynamic analysis of TCDD-induced cytochrome P450 gene expression in multiple tissues: Dose- and time-dependent effects. *Toxicol. Appl. Pharmacol.* **151**, 294–310.

Setoguchi, R., Hori, S., Takahashi, T., and Sakaguchi, S. (2005). Homeostatic maintenance of natural Foxp3(+) CD25(+) CD4(+) regulatory T cells by interleukin (IL)-2 and induction of autoimmune disease by IL-2 neutralization. *J. Exp. Med.* **201**, 723–735.

Thellin, O., Zorzi, W., Lakaye, B., De Borman, B., Coumans, B., Hennen, G., Grisar, T., Igout, A., and Heinen, E. (1999). Housekeeping genes as internal standards: Use and limits. *J. Biotechnol.* **75**, 291–295.

Van den Berg, M., Birnbaum, L., Bosveld, A. T., Brunstrom, B., Cook, P., Feeley, M., Giesy, J. P., Hanberg, A., Hasegawa, R., Kennedy, S. W., *et al.* (1998). Toxic equivalency factors (TEFs) for PCBs, PCDDs, PCDFs for humans and wildlife. *Environ. Health Perspect.* **106**, 775–792.

Veldhoen, M., Hirota, K., Westendorf, A. M., Buer, J., Dumoutier, L., Renauld, J. C., and Stockinger, B. (2008). The aryl hydrocarbon receptor links TH17-cell-mediated autoimmunity to environmental toxins. *Nature* **453**, 106–109.

Vorderstrasse, B. A., Cundiff, J. A., and Lawrence, B. P. (2004). Developmental exposure to the potent aryl hydrocarbon receptor agonist 2,3,7,8-tetrachlorodibenzo-p-dioxin impairs the cell-mediated immune response to infection with influenza a virus, but enhances elements of innate immunity. *J. Immunotoxicol.* **1**, 103–112.

Wheeler, J. L., Martin, K. C., Resseguie, E., and Lawrence, B. P. (2014). Differential consequences of two distinct AhR ligands on innate and adaptive immune responses to influenza A virus. *Toxicol. Sci.* **137**, 324–334.